IEEE Access
Multidisciplinary ⋮ Rapid Review ⋮ Open Access Journal

Received 2 May 2024, accepted 26 May 2024, date of publication 28 May 2024, date of current version 15 July 2024.

Digital Object Identifier 10.1109/ACCESS.2024.3406927

RESEARCH ARTICLE

Deep Learning Model for Magnetic Flux Density Prediction in Magnetic Spring on the Vibration Generator

GRAZIA LO SCIUTO[1,2], JOANNA BIJAK[1], ZYGMUNT KOWALIK[1], PAWEŁ KOWOL[1], RAFAŁ BROCIEK[3], AND GIACOMO CAPIZZI[2,3]

[1]Department of Mechatronic, Faculty of Electrical Engineering, Silesian University of Technology, 44-100 Gliwice, Poland
[2]Department of Electrical, Electronics and Informatics Engineering, University of Catania, 95125 Catania, Italy
[3]Department of Mathematics Applications and Methods for Artificial Intelligence, Faculty of Applied Mathematics, Silesian University of Technology, 44-100 Gliwice, Poland

Corresponding author: Rafał Brociek (rafal.brociek@polsl.pl)

This work was supported by the Silesian University of Technology, Poland, through the "Initiative of Excellence—Research University" Program.

ABSTRACT The magnetic spring placed on vibration generator consists of top and bottom fixed magnets with a third magnet levitated between them. Nonlinear dynamic analysis appears in the magnetic flux density of the magnetic spring activated by the vibration generator. This paper is focused on fast data-driven and accurate model for the prediction of magnetic flux density using a deep neural network (DNN) in the form of a Long Short-Term Memory (LSTM). As the input and training data for LSTM are used: supply voltage of the vibration generator, its frequency and measured magnetic flux density. The magnetic flux density measurements of the magnetic spring have been recorded by three Hall effect sensors. The prediction of magnetic flux density in magnetic spring has given accurate results and good applicability for better characterization of the device in energy harvesting system.

INDEX TERMS Deep learning, magnetic flux density, magnetic spring, energy harvesting, vibration.

NOMENCLATURE

$\hat{\boldsymbol{C}}_t$	New cell state vector.
$\boldsymbol{b}_c$	Bias matrices of new cell state.
$\boldsymbol{b}_i$	Bias matrices of input gate.
$\boldsymbol{b}_o$	Bias matrices of output gate.
$\boldsymbol{C}_t$	Current cell state.
$\boldsymbol{C}_{t-1}$	Previous cell state.
$\boldsymbol{f}_t$	Forget gate vector.
$\boldsymbol{h}_{t-1}$	Hidden state vector from previous cell.
$\boldsymbol{i}_t$	Input gate.
$\boldsymbol{o}_t$	Output gate.
$\boldsymbol{W}_c$	Weight matrices of new cell state.
$\boldsymbol{W}_i$	Weight matrices of input gate.
$\boldsymbol{W}_o$	Weight matrices of output gate.
$\boldsymbol{x}_t$	Input vector at particular time.
ρ	Mass density of magnet.
σ	Activation binary sigmoid function.
B	Magnetic flux density.
B_r	Remanence of magnet.
BH_{max}	Maximum energy product.
F_m	Approximated spring force of magnetic spring.
f_r	Resonance frequency.
f_s	Sampling frequency.
f_{cut}	Cutoff frequency.
$H(s)$	Transmittance of Butterworth filter.
H_{cB}	Normal coercivity of magnet.
H_{cJ}	Intrinsic coercivity of magnet.
k_n	n^{th} coefficient of polynomial of the approximation of the magnetic spring.
m_m	Middle magnet mass.
n	Natural number.
s	Complex frequency.
$tanh$	Activation tangents hyperbolic function.

The associate editor coordinating the review of this manuscript and approving it for publication was Sandra Costanzo.

V_o Measured output voltage.
V_{offset} Offset voltage.
z Displacement of middle magnet.

I. INTRODUCTION

Energy consumption and environmental pollution from fossil fuel extraction have led to the investigation and optimization of new energy harvesting solutions and devices [1], [2], [3], [4]. For small electronic devices, the most common energy sources are considered solar panels and vibration energy harvesters that use piezoelectric, electrostatic, and electromagnetic technologies [3], [5], [6], [7], [8]. Recently the magnetic springs are considered the promising devices in energy harvesting system for magnetic and mechanical properties. Magnetic springs are a fatigue-free alternative to mechanical springs and have the potential to enable compliant actuation concepts in highly dynamic industrial applications, more durable than the conventional mechanical springs and can be conveniently adjusted to the required force [9].

Magnetic spring is a set of permanent magnets that repel each other. The repulsive force is considered spring force, because it allows to store the energy when magnets are brought close together - spring is compressed. The energy is then released when the magnets move away - spring is stretched [10]. The spring force of the magnetic spring is nonlinear and highly depends on the magnetic properties of the magnetic spring components and their configuration [11], [12], [13], [14]. In energy harvesting application magnetic spring is used as the mechanism that hold moving magnet inside the coil. The optimization of such magnetic spring focuses mainly on the magnetic spring forces and the arrangement of the coils around the magnetic spring [11], [12], [13], [15], [16]. The optimum coils arrangement depends on the magnetic field distribution, especially during the magnet movement [17], [18]. The dynamical simulations to compute 3D or 2D dimensional magnetic field in magnetic spring require too time-consuming for fast iterations. To investigate the characteristics of magnetic fields in many real applications is important to require measurements or simulations and guarantee low time-consuming. For fast analysis of distribution of the magnetic field is considered the machine learning including neural network. The prediction of magnetic field value at a random point in space from a few point measurements was performed using a generative adversarial network structure linear compared to conventional methods such as linear interpolation, splines, and biharmonic equations [19]. In [20] the feed-forward neural networks were used to estimate electric field intensity and magnetic flux density for different overhead transmission line configurations allowing to reduce time for optimization. Machine learning in the field of magnetism can reduce the computational load and support the characterization of magnetic field measurements [21], [22], [23]. The authors have proposed the design and analysis of the magnetic spring and vibration generator, measurements of magnetic flux density conducted on the magnetic spring prototype, and the deep learning model for the prediction of the magnetic flux density in the magnetic spring excited by the vibration generator. The open-loop prediction predicts the next time step of a sequence of magnetic flux densities using only the input data of magnetic flux densities of magnetic spring, voltages and frequencies of vibration generator. The average RMSEs over all test observations for magnetic density of lower, middle and upper sensors are respectively 4.58 %, 0.75 % and 4.67 %. In this type of applications, high and fast predictive accuracy and low errors are achieved.

The model-based prediction of the magnetic flux density can support the characterization and optimization of the magnetic spring, which in turn could enhance the usefulness of such devices in energy harvesting applications.

This paper is organized as follows: in Section II, the magnetic spring and vibration generator are briefly described, and the measurements of magnetic flux density are analyzed in Section III. The deep learning method is introduced and modelled in Section IV. Conclusions are summarized in Section VI.

A. MAIN CONTRIBUTIONS

This study will contribute to the growing development and optimization of magnetic spring energy harvesting system. The model-based prediction of the magnetic flux density can support the characterization and optimization of the magnetic spring, which in turn could enhance the usefulness of such devices in energy harvesting applications. More particularly, the main contributions are summarized as follows:

- The paper proposes the design and analysis of the magnetic spring and vibration generator.
- In the first step measurements of magnetic flux density have been conducted on the magnetic spring prototype.
- The time-domain magnetic density flux signal was analyzed using low-pass Butterworth filter.
- The prediction method based on long short-term memory (LSTM) networks for magnetic flux density is proposed.
- The deep learning model for the prediction of the magnetic flux density in the magnetic spring excited by the vibration generator was achieved.
- The open-loop prediction predicts the next time step of a sequence of magnetic flux densities using just the input data such as the magnetic flux densities of magnetic spring, voltages and frequencies of vibration generator.

This paper is organized as follows: in Section II, the magnetic spring and vibration generator are briefly described, and the measurements of magnetic flux density are analyzed in Section III. The deep learning method is introduced and modelled in Section IV. Discussion and conclusions are summarized in Section V and VI, respectively.

II. DESIGN AND MODELING

A. LABORATORY STAND

Laboratory stand was developed at the laboratory of the Department of Mechatronics, the Silesian University of

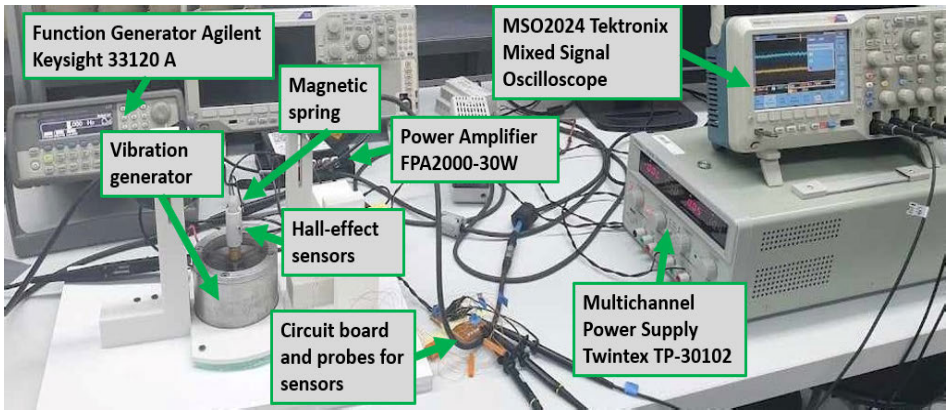

FIGURE 1. Laboratory stand for measurement of the magnetic flux density in the magnetic spring.

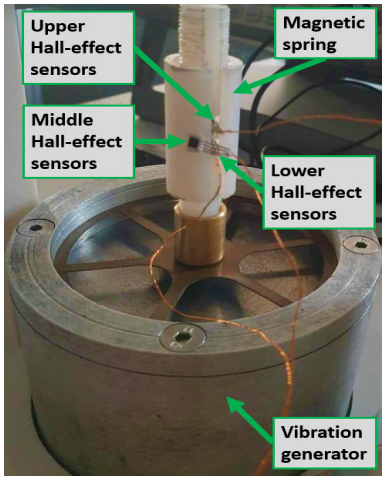

FIGURE 2. Vibration generator, magnetic spring and the Hall-effect sensors.

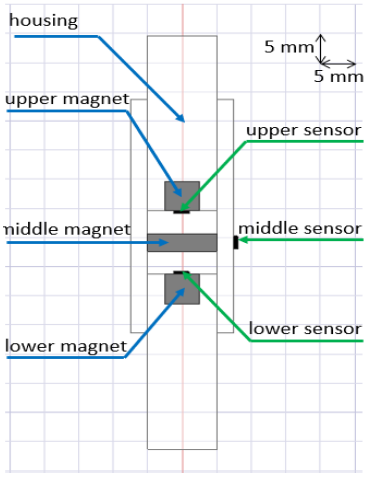

FIGURE 3. Hall-effect sensor mounted on the magnetic spring.

Technology, Gliwice, Poland in order to measure the dynamical changes in the magnetic flux density of the vibrating magnetic spring (Fig. 1). It was equipped for the conducted measurements by the instruments such as: vibration generator, magnetic spring, Hall-effect sensors CYSJ362 A, function generator Agilent Keysight 33210A, Power Amplifier FPA2000-30W, Multichannel Power Supplies TWINTEX TP-30102 and MSO2024 Tektronix Mixed Signal Oscilloscope.

The vibration generator is controlled and powered by the signal from the function generator Agilent Keysight 33120A amplified by the Power Amplifier FPA2000-30W. The magnetic spring is mounted on the vibration generator as shown in Fig. 2.

The movement of the magnetic spring is induced by the vibration generated by the vibration generator. The three Hall-effect sensors CYSJ362 A are supplied by Multichannel Power Supplies TWINTEX TP-30102. The measurement of the output voltage for the Hall-effect sensors are conducted by means of the MSO2024 Tektronix Mixed Signal Oscilloscope with the sample cycle 1.6 μs.

1) VIBRATION GENERATOR

Electromagnetic vibration generators are used in printing and packaging technology, as well as in the pharmaceutical industry, generate oscillating vibrations. The vibration generator manufactured in the laboratory generates mechanical vibration and consists of the ring permanent magnet between two steel fastening rings, the rod with the coil and the magnetic steel circuit enclosed in the aluminum housing. The two membranes are placed on the bottom and top part of the housing. Alternating voltage of the specified frequency applied to the coil, causes the movement of the rod and the membranes for the same frequency.

The ring permanent magnet is a sintered ferrite magnet (F30) with a height of 12 *mm*, an outer diameter of 80 *mm* and an inner diameter of 40 *mm*. The most important magnetic, physical and technical characteristics of commercially available magnet materials are stated by the manufacturer ([24]) as follows:

- Coercivity H_{cB} min. 175 kA/m
- Coercivity H_{cJ} min. 180 kA/m
- Energy product (BH_{max}) min. 26 $kJ/m3$

TABLE 1. Coefficients of force polynomial.

k_9	-3.96×10^{21}	k_6	-13.21	k_3	-7.06×10^{5}
k_8	4.27×10^{5}	k_5	-1.03×10^{12}	k_2	-3.66×10^{-10}
k_7	4.11×10^{16}	k_4	1.23×10^{-4}	k_1	527.05

- Remanence B_r 0.37 T
- Density ρ 4.5 g/cm_3

The fastening rings have the inner and outer diameter matched with the ring magnet and a height of 7 *mm* for the top fastening ring and 10 *mm* for the bottom one. The cylindrical coil is made of copper wire with a diameter of 0.3 *mm* and a length of 32.5 *mm* has 280 number of turns, a height of 17.5 *cm*, an outer and inner diameter of 35 *mm* and 39 *mm* respectively.

2) MAGNETIC SPRING

The magnetic spring is settled on top of the vibration generator and is moved by vibration as shown in the Fig. 2. It consists of three cylindrical neodymium magnets that are assembled in a cylindrical polyamide casing at the laboratory. The magnets are axially aligned and set up to repel each other. The two external magnets are fixed to the screw element of the housing, allowing the position to be determined before the performing measurement. The middle magnet can freely levitate between the fixed magnets. The magnetic and physical properties of the neodymium magnets N38 (NdFeB) are given by the producer [25] as follows:

- Coercivity H_{cB} min. 899 kA/m
- Coercivity H_{cJ} min. 955 kA/m
- Energy product (BH_{max}) 286–302 kJ/m^3
- Remanence B_r 1.21–1.25 T
- Density ρ 7.5 g/cm^3.

The outer magnets have diameters and heights of 5 *mm*, and the middle magnet has diameter of 10 *mm* and a height of 3 *mm*. The spacing between top and bottom magnets is 11 *mm*.

The repulsive force of the magnets is the spring force and depends on their magnetic properties and the distance between the magnets. Thus the spring force of the magnetic spring is non-linear and depends on the position of the middle magnet. The approximation relation of the measured spring force of the magnetic spring is described in (1) by 9^{th} degree polynomial.

$$F_m = \sum_{n=1}^{9} k_n z^n \tag{1}$$

where k_n is the n^{th} coefficient of polynomial and z is the displacement of the middle magnet. The coefficients are given in the Table 1.

3) HALL-EFFECT SENSOR

Magnetic sensors have been used for the detection of magnetic flux density in the magnetic device. For the purpose of detecting the presence and magnitude of a magnetic field, three Hall-effect sensors CYSJ362 A made of mono-crystal gallium arsenide (GaAs) semiconductor material group III-V have been mounted on the magnetic spring's casing in proximity of the upper, middle, and lower magnets (Fig. 3).

The Hall-effect sensors are connected between printed circuit board, capacitors of 4.7 μF and 100 nF, voltage supply sets to 10.4 V and current sets to 0.05 A. The magnetic flux density is proportional to the output voltage detected by the Hall-effect sensors, affected by the temperature and supply voltage [26]. The magnetic flux density at the temperature of 20 °C and for the supply voltage of 10 V can be calculated from (2).

$$B = \frac{1}{3.13333}(V_o - V_{offset}) \tag{2}$$

where V_o is the measured output voltage, V_{offset} is the offset voltage.

III. MEASUREMENTS

A. MAGNETIC FLUX DENSITY MEASUREMENT

The magnetic flux density distribution in magnetic spring depends on amplitude and frequency of vibrating source. The magnetic flux density change is crucial for energy generation of the magnetic spring.

Magnetic flux density measurements in the magnetic spring were carried out to set six input voltages V_{in} equal to 1 V, 2 V, 3 V, 4 V, 5 V and 6 V and frequencies f from 0 to 120 Hz using an Agilent Keysight 33120A function generator connected to the vibration generator.

Output voltage of the sensors measured with the MSO2024 Tektronix Oscilloscope was further converted to the magnetic flux density by (2). The time-domain magnetic density flux signals were low-pass filtered using the Butterworth filter. The 2^{nd} order filter was designed for the data sampled with the frequency f_s set to 62.5 kHz and for the cutoff frequency f_{cut} set to 2 kHz. The transmittance of the designed filter is given in (3).

$$H(s) = \frac{9.96 \times 10^{-5}s^2 + 1.99 \times 10^{-4}s + 9.96 \times 10^{-5}}{s^2 - 1.97s + 0.97} \tag{3}$$

B. MAGNETIC FLUX DENSITY IN MAGNETIC SPRING

1) MAGNETIC SPRING RESONANCE FREQUENCY

The magnetic flux density measurements results in time series detected by the lower, middle and upper sensors for each voltages set on the function generator V_{in} are shown respectively in Fig. 4 (a), Fig. 4 (b), Fig. 4 (c) at a frequency of 85 Hz. This frequency is considered the main resonance frequency of the magnetic spring, emphasizing the behavior of a magnetic spring in terms of the physical phenomena that occurs when the magnet is subjected to external vibration that corresponds its natural frequency. In the conducted measurement tests, two resonance frequency of the magnetic spring were confirmed not only at 85 Hz but also at 110 Hz. The first one is due to the linear movement of the middle magnet in magnetic spring [27]. It is derived specifically by

the following equation (4):

$$f_r = \sqrt{\frac{k_1}{m_m}} \tag{4}$$

where m_m is the mass of the middle magnet, k_1 is the 1^{st} coefficient of polynomial reported in (1). The second frequency is a result of the rotation of the middle magnet during the movement as reported in [27], [28], and [29].

The resonance frequency of a magnetic spring plays an important role for industrial applications in the energy harvesting from environmental vibrations i.e. wind, tidal waves, vehicles, and human motions, and from industrial machinery vibrations. The magnetic spring can be used as the clamping mechanism in the electromagnetic energy harvester in order to work at the resonance frequency for the highest output power.

2) MAGNETIC FLUX DENSITY RESULTS

In Fig. 4 (a) the measured values of the magnetic flux density detected by the lower sensor in time series for each voltages set on the function generator V_{in} are varying in the range of 149 mT and 157 mT. In Fig. 4(b) the measured values of the magnetic flux detected by the middle sensor are in the range from 145 mT to 151 mT. In Fig. 4(c) the measured values of the magnetic flux detected by the upper sensor are in the range from 130 mT to 142 mT.

Due to the movement of the middle magnet, the amplitude of the magnetic flux density detected by the lower sensor on the magnetic spring is higher than the magnetic flux density detected by middle and upper sensors. The average position of the middle magnet is closer to the lower magnet because of the gravitational force, which results in the increase of the magnetic field near lower sensor.

The maximum value of the magnetic flux density, near 156 mT, is detected by the lower sensor for the 1 V, caused by the middle magnet proximity. In Fig. 4 (a) and (b) the measured magnetic flux densities detected by the lower and middle sensors for the 3 V and 4 V are lower than magnetic flux density for the other voltages, caused by the demagnetization of the magnetic spring. For the voltages of 3, 5 and 6 V there is significant rise in the magnetic flux density amplitude caused by the higher amplitude of the middle magnet movement for the resonance frequencies of the magnetic spring (85 Hz). The values of the magnetic flux density detected by the upper sensor in time series for each voltages set on the function generator V_{in} are similar for each frequency (Fig. 4(c)). For the voltages from 2 V to 6 V values vary from 138 mT to 142 mT. For 1 V magnetic flux density value is lower (130 mT - 132 mT), due to the low amplitude of the external vibration of magnetic spring.

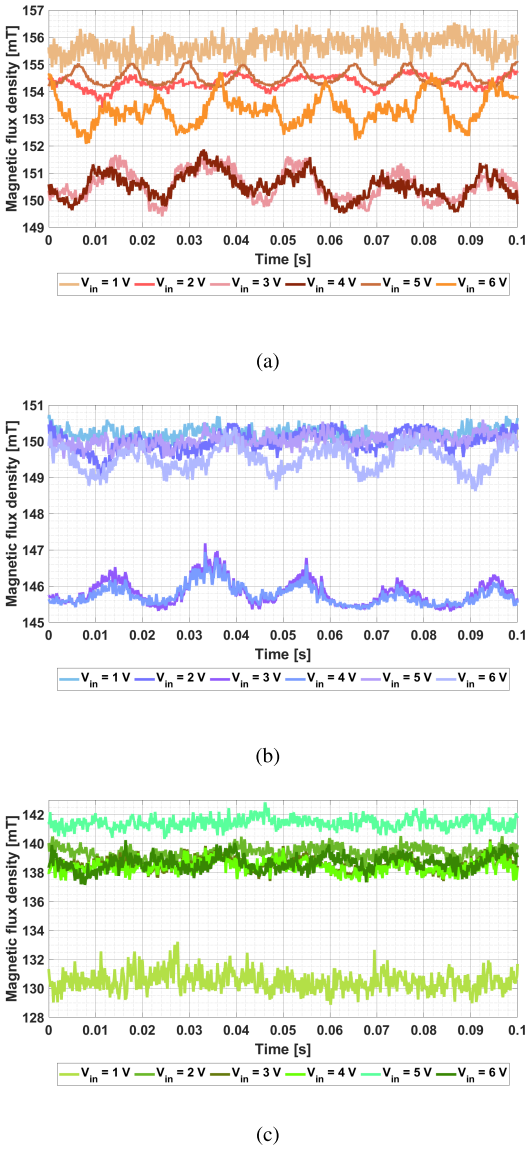

FIGURE 4. Magnetic flux density detected for the frequency of 85 Hz by (a) the lower sensor, (b) the middle sensor and (c) the upper sensor.

IV. METHODS

A. DEEP-LEARNING

Machine learning algorithms are considered data-driven with data originated from measurements or simulations. The deep learning is the mapping of input data to the output domain inspired to the biological neural network structure. A neural network consists of multiple parameter layers that can be trained to extract higher-level features. During the process of optimization, the parameters are updated to minimize the difference between a given output and the predicted value based on the input dataset. Deep learning performs efficiently complex computations on vast amounts of data using specific structures and functions. In particular it focuses on using more complex neural networks to recognize the relationships between different inputs by observing hidden data structures. Recurrent neural networks (RNNs) include long short-term memory networks (LSTM). Due to their ability to understand long-term connections between data time steps. A long short-term memory network is a type of recurrent neural network (RNN) frequently used to process, analyze, predict

and classify sequential time-series data. The LSTM models were developed to introduce memory or cell states into the network. In this case, the cell state is considered as a container in which the information can be added, removed and stored over the time. The complex LSTM network structure has different cell blocks connected in series. Each LSTM cell consists of three gate blocks that control its state (input gate, forget gate and output gate). The LSTM gates make small changes to the information flowing through the network by multiplying, deleting, and adding from memory cells. A gate is a classical neural network consisting of weights, biases, and activation functions. A memory cell is controlled by three gates (Fig. 5):

- The forget gate controls and removes useless information from memory cells. The two input variables applied to the gate are: $\boldsymbol{h}_{t-1}$ that is the hidden state vector from the previous cell, and $\boldsymbol{x}_t$ is the input vector at the particular time. The same inputs are multiplied by the weight matrices ($\boldsymbol{W}_i$ and followed by the bias $\boldsymbol{b}_f$). Following this, the binary sigmoid function (σ) is applied to the resultant as described in (5). In particular, if the output value for a memory state is "0", the information is forgotten; if the output value is "1" the information is kept for future use.

$$\boldsymbol{f}_t = \sigma(\boldsymbol{W}_i \cdot [\boldsymbol{h}_{t-1}, \boldsymbol{x}_t] + \boldsymbol{b}_f) \tag{5}$$

- The input gate controls and updates the addition of information to the cell states. First, the information is adjusted by the sigmoid function. This function acts as a filter for all inputs $\boldsymbol{h}_{t-1}$ and $\boldsymbol{x}_t$. Then, a vector is created containing all possible values of the input, using a tan hyperbolic function *tanh* that gives an output from -1 to +1. The equations for the input gate vector and for the new cell state vector are described in (6) and in (7), respectively.

$$\boldsymbol{i}_t = \sigma(\boldsymbol{W}_i \cdot [\boldsymbol{h}_{t-1}, \boldsymbol{x}_t] + \boldsymbol{b}_i) \tag{6}$$

$$\hat{\boldsymbol{C}}_t = tanh(\boldsymbol{W}_c \cdot [\boldsymbol{h}_{t-1}, \boldsymbol{x}_t] + \boldsymbol{b}_c) \tag{7}$$

where *tanh* is the activation function, $\boldsymbol{W}_i$ is weight matrices of input gate, $\boldsymbol{b}_i$ is bias matrices of input gate, $\boldsymbol{W}_c$ is weight matrices of new cell state, $\boldsymbol{b}_c$ is bias matrices of new cell state.

The current cell state is result of the Hadamard multiplication of the forget gate and previous cell state $\boldsymbol{C}_{t-1}$ and the input gate and new cell state, shown in (8).

$$\boldsymbol{C}_t = \boldsymbol{f}_t .* \boldsymbol{C}_{t-1} + \boldsymbol{i}_t .* \hat{\boldsymbol{C}}_t \tag{8}$$

where the operator $.*$ defines the Hadamard multiplication or element-wise.

- The output gate is used to control which useful information from the current hidden state is considered as output. First, a vector is created after applying *tanh* function to the memory cell. Then, the filter of sigmoid function can regulate the inputs $\boldsymbol{h}_{t-1}$ and $\boldsymbol{x}_t$. At last, the values of the vector and the regulated values are multiplied to be sent as an output and also to the hidden state of the next cell. The equation for the output gate vector is (9).

$$\boldsymbol{o}_t = \sigma(\boldsymbol{W}_o \cdot [\boldsymbol{h}_{t-1}, \boldsymbol{x}_t] + \boldsymbol{b}_o) \tag{9}$$

where $\boldsymbol{W}_o$ is weight matrices of output gate, $\boldsymbol{b}_o$ is bias matrices of output gate.

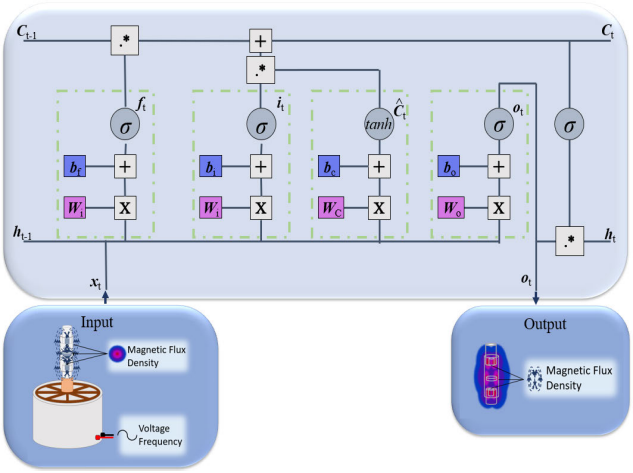

FIGURE 5. LSTM architecture.

B. RESULTS AND PREDICTIONS OF MAGNETIC FLUX DENSITY BASED ON LSTM MODEL

The open-loop prediction predicts the next time step of a sequence of magnetic flux densities using only the input data. The magnetic flux historical dataset is divided into training, verification and test dataset to verify the performance of LSTM model. The value of magnetic flux density is predicted for time step t of the sequence using data collected at time steps 1 to $t-1$ (Fig. 5). The artificial neural network for learning architecture, in the form of a Long Short-Term Memory (LSTM) network is particularly well suited for time series of magnetic flux density in the magnetic spring. The inputs of neural network LSTM are considered the magnetic flux density, the frequency and voltage. The output is the magnetic flux density at 150 time step forward.

The neural network LSTM designer has the sequence Input Layer with input Size of 3.

The number of hidden units that refers to the dimensionality is 140. The state activation function that controls the flow of information and gradients is 'tanh'(hyperbolic tangent), and gate activation function is a 'sigmoid'.

A fully connected Layer, that takes the inputs from the feature analysis and applies weights to predict the correct label, has input Size of 140 and output Size of 140.

The specify training options have included the Adam optimization and the train for 50 epochs. The observations for training used in the neural network are about 70% and the rest for testing/validation.

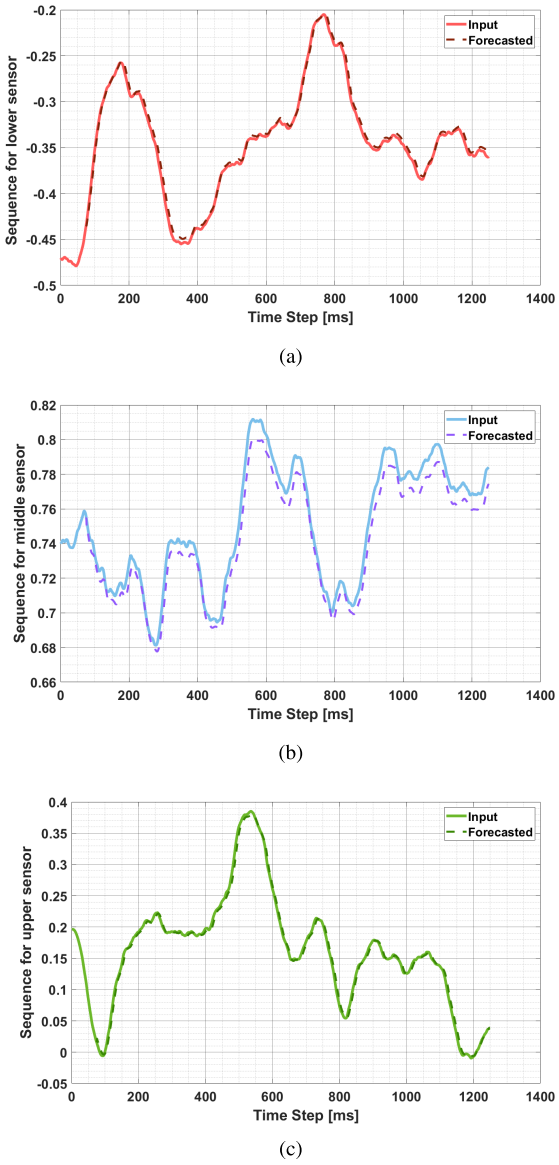

FIGURE 6. Tests of sequences for the prediction of magnetic flux density conducted for (a)lower sensor(b) middle sensor (c) upper sensor.

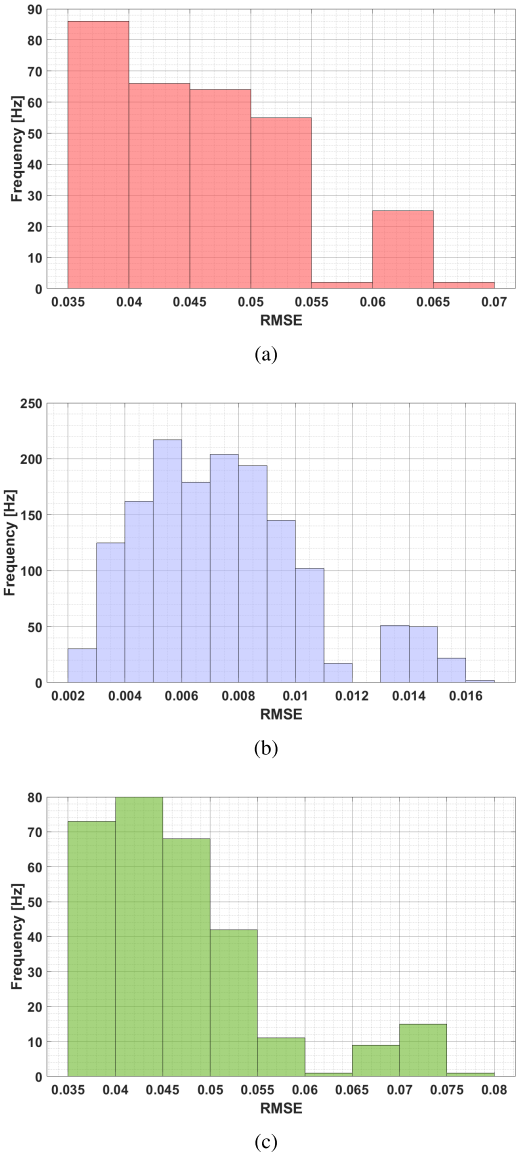

FIGURE 7. Error histogram of magnetic flux density conducted for (a) lower sensor(b) middle sensor (c) upper sensor.

The current and previous sequences data input of neural network LSTM network (magnetic flux densities, voltages and frequencies) and the predicted values are shown in the Fig.6(a), Fig.6(b) and Fig.6(c). The forecast time series data using long short-term memory network were obtained in Deep Network Designer implemented in Matlab. For each prediction, use the previous prediction as the input to the function. The test of the current and previous sequences of neural network LSTM (magnetic flux densities, voltages and frequencies) and the predicted values are shown in the Fig.6(a), Fig.6(b) and Fig.6(c). To evaluate the accuracy for each test sequence, the root mean square error (RMSE) was calculated between the predictions and the target. The average RMSEs over all test observations for magnetic density of lower, middle and upper sensors are respectively 0.0458, 0.0075 and 0.0467. The errors are very low for each sequences indicating the greater accuracy as shown in the histograms Fig.7(a),Fig.7(b),Fig.7(c).

V. DISCUSSION

The magnetic flux density distributions are usually determined by the Finite Elements Method (FEM) models, however in the energy harvesting system based on magnetic spring, the demagnetization of the magnets cannot be estimated with high performance. In [29] the 2D FEM model of magnetic spring on the vibration generator exhibits an error of magnetic flux density of 20% compared to the measurements conducted in the laboratory. In addition the dynamical simulation of the magnetic field distribution and the magnetic spring movement induced by the external

vibration requires complex, time-consuming calculations, hence making troublesome the model development of the inertial system. On the other hand the lower computation time in the analysis of the magnetic flux density can be achieved by LSTM network model. The magnetic flux density can be predicted without the definition of the mechanical parameters of the magnetic spring and vibration generator. LSTM can overcome short-term memory problems, non linearity and demagnetization effectively. In LSTM prediction the average RMSEs over all test observations for magnetic density is 4.6 %. Thus, the accuracy of the LSTM neural network can be considered a good solution for prediction of magnetic density with low error, fast training of dataset and superior performance, which is especially useful in the optimization process of the device.

VI. CONCLUSION

The neural network LSTM has been developed for the magnetic flux density predictions of magnetic spring excited by the vibration generator. Experimental measurement tests of magnetic flux density have been conducted in laboratory in order to determine the magnetic distribution of magnetic spring. The predictive model based on LSTM is fast and accurate. It can be useful and profitable for characterization and optimization of magnetic spring in the energy harvesting applications in order to achieve highest power generated by the spring or highest efficiency of such generator.

In the future work this computational model can be extended for various combination of the magnets in magnetic spring for the analysis and control of the resonance frequency. Hence, in the system design could be included and developed the real-time control hardware through a microcontroller and system-design platform.

REFERENCES

[1] J. Mohtasham, "Renewable energies," *Energy Proc.*, vol. 74, pp. 1289–1297, Jan. 2015.
[2] D. Gielen, F. Boshell, D. Saygin, M. D. Bazilian, N. Wagner, and R. Gorini, "The role of renewable energy in the global energy transformation," *Energy Strategy Rev.*, vol. 24, pp. 38–50, Apr. 2019.
[3] M. Li, A. Luo, W. Luo, and F. Wang, "Recent progress on mechanical optimization of MEMS electret-based electrostatic vibration energy harvesters," *J. Microelectromech. Syst.*, vol. 31, no. 5, pp. 726–740, Oct. 2022.
[4] M. R. Sarker, S. Julai, M. F. M. Sabri, S. M. Said, M. M. Islam, and M. Tahir, "Review of piezoelectric energy harvesting system and application of optimization techniques to enhance the performance of the harvesting system," *Sens. Actuators A, Phys.*, vol. 300, Dec. 2019, Art. no. 111634.
[5] P. Malaji, S. Ali, and G. Litak, "Energy harvesting: Materials, structures and methods," *Eur. Phys. J. Special Topics*, vol. 231, pp. 1355–1358, 2022, doi: 10.1140/epjs/s11734-022-00578-7.
[6] P. B. Rathod, N. Makandar, K. Suguresh, V. Harage, and P. V. Malaji, "Analysis of energy harvesting from human motion," in *Proc. IEEE North Karnataka Subsection Flagship Int. Conf. (NKCon)*, Nov. 2022, pp. 1–5.
[7] K. T. Prajwal, K. Manickavasagam, and R. Suresh, "A review on vibration energy harvesting technologies: Analysis and technologies," *Eur. Phys. J. Special Topics*, vol. 231, no. 8, pp. 1359–1371, Jul. 2022.
[8] A. Khaligh, P. Zeng, and C. Zheng, "Kinetic energy harvesting using piezoelectric and electromagnetic technologies—State of the art," *IEEE Trans. Ind. Electron.*, vol. 57, no. 3, pp. 850–860, Mar. 2010.
[9] B. Mrak, B. Lenaerts, W. Driesen, and W. Desmet, "Optimal magnetic spring for compliant actuation—Validated torque density benchmark," *Actuators*, vol. 8, no. 1, p. 18, Feb. 2019.
[10] K.-X. Qian, P. Zeng, W. Ru, and H.-Y. Yuan, "Novel magnetic spring and magnetic bearing," *IEEE Trans. Magn.*, vol. 39, no. 1, pp. 559–561, Jan. 2003.
[11] J. Bijak, T. Trawiński, and M. Szczygieł, "Simulation and investigation of the change of geometric parameters on voltage induced in the energy harvesting system with magnetic spring," *Electronics*, vol. 11, no. 10, p. 1639, May 2022.
[12] Q. Zhang, Y. Wang, and E. S. Kim, "Electromagnetic energy harvester with flexible coils and magnetic spring for 1–10 Hz resonance," *J. Microelectromech. Syst.*, vol. 24, no. 4, pp. 1193–1206, Aug. 2015.
[13] W. Wang, J. Cao, N. Zhang, J. Lin, and W.-H. Liao, "Magnetic-spring based energy harvesting from human motions: Design, modeling and experiments," *Energy Convers. Manage.*, vol. 132, pp. 189–197, Jan. 2017.
[14] J. Enayati and P. Asef, "Review and analysis of magnetic energy harvesters: A case study for vehicular applications," *IEEE Access*, vol. 10, pp. 79444–79457, 2022.
[15] T. Wang, Z. Zhu, and S. Zhu, "Comparison of vibration energy harvesters with fixed and unfixed magnetic springs," *Electron. Lett.*, vol. 54, no. 10, pp. 646–647, May 2018.
[16] T. Wang and S. Zhu, "Resonant frequency reduction of vertical vibration energy harvester by using negative-stiffness magnetic spring," *IEEE Trans. Magn.*, vol. 57, no. 9, pp. 1–7, Sep. 2021.
[17] M. Hasani and M. I. Rahaghi, "The optimization of an electromagnetic vibration energy harvester based on developed electromagnetic damping models," *Energy Convers. Manage.*, vol. 254, Feb. 2022, Art. no. 115271.
[18] D. Spreemann, D. Hoffmann, B. Folkmer, and Y. Manoli, "Numerical optimization approach for resonant electromagnetic vibration transducer designed for random vibration," *J. Micromech. Microeng.*, vol. 18, no. 10, Oct. 2008, Art. no. 104001.
[19] S. Pollok, N. Olden-Jørgensen, P. S. Jørgensen, and R. Bjørk, "Magnetic field prediction using generative adversarial networks," *J. Magn. Magn. Mater.*, vol. 571, Apr. 2023, Art. no. 170556.
[20] A. Alihodzic, A. Mujezinovic, and E. Turajlic, "Electric and magnetic field estimation under overhead transmission lines using artificial neural networks," *IEEE Access*, vol. 9, pp. 105876–105891, 2021.
[21] V. Mateev and I. Marinova, "Machine learning in magnetic field calculations," in *Proc. 19th Int. Symp. Electromagn. Fields Mechatronics, Electr. Electron. Eng. (ISEF)*, Aug. 2019, pp. 1–2.
[22] H. Wu, Y. Zhang, W. Fu, C. Zhang, and S. Niu, "A novel pre-processing method for neural network-based magnetic field approximation," *IEEE Trans. Magn.*, vol. 57, no. 10, pp. 1–9, Oct. 2021.
[23] A. Khan, V. Ghorbanian, and D. Lowther, "Deep learning for magnetic field estimation," *IEEE Trans. Magn.*, vol. 55, no. 6, pp. 1–4, Jun. 2019.
[24] *Top Magnesy*. Accessed: Feb. 12, 2024. [Online]. Available: https://topmagnesy.com/pl/magnesy-ferrytowe-pierscieniowe/1300-magnes-ferrytowy-pierscieniowy-mp-80x40x12-f30.html
[25] *ENES Magnesy*. Accessed: Feb. 12, 2024. [Online]. Available: https://enesmagnets.pl/en/permanent-magnets/neodymium-sintered/cylindrical-magnets/
[26] *Chenyang Technologies*. Accessed: Feb. 12, 2024. [Online]. Available: https://www.chenyang-gmbh.com/en/linear-hall-effect-sensors-elements-cysj362a-max.-sensitivity-3.1-4.1-mv/mt-measuring-range-3t.html
[27] J. Bijak, G. Lo Sciuto, Z. Kowalik, T. Trawiński, and M. Szczygieł, "A 2-DoF kinematic chain analysis of a magnetic spring excited by vibration generator based on a neural network design for energy harvesting applications," *Inventions*, vol. 8, no. 1, p. 34, Jan. 2023.
[28] G. L. Sciuto, J. Bijak, Z. Kowalik, M. Szczygieł, and T. Trawiński, "Displacement and magnetic induction measurements of energy harvester system based on magnetic spring integrated in the electromagnetic vibration generator," *J. Vibrat. Eng. Technol.*, vol. 12, no. 3, pp. 3305–3320, Mar. 2024.
[29] J. Bijak, G. Lo Sciuto, Z. Kowalik, P. Lasek, M. Szczygieł, and T. Trawiński, "Magnetic flux density analysis of magnetic spring in energy harvester by Hall-effect sensors and 2D magnetostatic FE model," *J. Magn. Magn. Mater.*, vol. 579, Aug. 2023, Art. no. 170796.

GRAZIA LO SCIUTO received the Laurea degree in electronic engineering from the University of Catania, Catania, Italy, in 2006, and the Ph.D. degree in applied electronics from the University of Rome Tre, Rome, Italy, in 2017. She has worked for several different companies (i.e. Air Liquide, NBC filters Company, Numidia s.r.l., and the Department of Regional Ministry of Agriculture and Forestry), from 2007 to 2012. From 2014 to 2018, she was a Researcher with the Optoelectronic Organic Semiconductor Devices Laboratory, Ben-Gurion University of the Negev, Be'er Sheva, Israel. From 2013 to 2023, she was a temporary Research Fellow with the University of Catania. She is currently an Assistant Professor with the Department of Mechatronics, Silesian University of Technology, Gliwice, Poland. Her current research interests include the development and investigation of electronic organic devices and sensors, innovative materials, renewable energy technologies, and soft computing techniques, such as artificial neural networks applied to complex systems and computational problems.

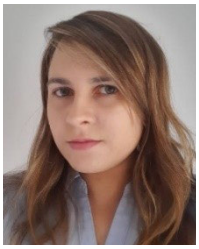

JOANNA BIJAK was born in Gliwice, Poland, in May 1994. She received the Master of Science degree in mechatronics from the Faculty of Electrical Engineering, Silesian University of Technology (SUT), Poland, in 2018, and the Ph.D. degree in electrical engineering. Currently, she is an Assistant Professor with the Department of Mechatronics, SUT. Her research interests include mathematical modeling, homogenous transformation, energy harvesting, and magnetic springs.

ZYGMUNT KOWALIK was born in Zabrze, Poland. He received the Engineering, M.Sc. Diploma, and Ph.D. degrees in mechatronics from the Faculty of Electrical Engineering, Silesian University of Technology (SUT), Gliwice, in 2012, 2013, and 2019, respectively. His Ph.D. thesis concerns the control algorithm of a synchronous reluctance machine. Currently, he is an Assistant Professor with the Department of Mechatronics, SUT. His research interests include mathematical modeling, electrical machines, and control theory and systems.

PAWEŁ KOWOL was born in Poland, in 1975. He received the M.S. and Ph.D. degrees from the Silesian University of Technology, Gliwice, Poland, in 2000 and 2007, respectively. Since 2005, he has been with the Department of Mechatronics, Silesian University of Technology. His current research interests include electromechanical devices, applications of magnetorheological fluid in mechatronic devices, and also haptic and tactile control systems of mechatronic systems.

RAFAŁ BROCIEK received the M.Sc. degree in mathematics from the Silesian University of Technology, Gliwice, Poland, in 2013, and the Ph.D. degree in technical sciences from Czestochowa University, in 2019. He is currently a Researcher with the Department of Mathematics Applications and Methods for Artificial Intelligence, Silesian University of Technology. His research interests include artificial intelligence, the application of computational methods to various problems in engineering, and mathematical simulation. He has experience in mathematical modeling, applying fractional calculus in engineering, and the application of artificial intelligence methods in optimization problems.

GIACOMO CAPIZZI received the Laurea degree (summa cum laude) in electronic engineering from the University of Catania, Catania, Italy, in 1993, and the Ph.D. degree in electronic and computer engineering from the University of Reggio Calabria, Reggio Calabria, Italy, in 2000. From 1993 to 1996, he was a Cabling Systems Designer with Itel. In 2022, he was an Associate Professor with the Department of Electrical, Electronics, and Informatics Engineering, University of Catania, where he joined as an Assistant Professor, in 2002. Since 2015, he has been a Lecturer with the Faculty of Applied Mathematics, Silesian University of Technology. He also teaches a master's course on the topic of algorithms and paradigms for pattern recognition. His research interests include wavelet theory, neural networks, statistical pattern recognition, Bayesian networks, theory and design of linear and nonlinear digital/analog filters, integrated generation systems, renewable energy sources, and battery storage modeling and simulation.